

# UC Santa Barbara

## UC Santa Barbara Previously Published Works

### Title

A universal design for a DNA probe providing ratiometric fluorescence detection by generation of silver nanoclusters

### Permalink

<https://escholarship.org/uc/item/71q03858>

### Journal

Nanoscale, 8(30)

### ISSN

2040-3364

### Authors

Del Bonis-O'Donnell, Jackson Travis  
Vong, Daniel  
Pennathur, Sumita  
[et al.](#)

### Publication Date

2016-08-14

### DOI

10.1039/c6nr03827a

Peer reviewed



Cite this: *Nanoscale*, 2016, 8, 14489

## A universal design for a DNA probe providing ratiometric fluorescence detection by generation of silver nanoclusters†

Jackson Travis Del Bonis-O'Donnell,\*‡<sup>a</sup> Daniel Vong,<sup>a</sup> Sumita Pennathur<sup>a</sup> and Deborah Kuchnir Fyngenson<sup>b</sup>

DNA-stabilized silver nanoclusters (AgNCs), the fluorescence emission of which can rival that of typical organic fluorophores, have made possible a new class of label-free molecular beacons for the detection of single-stranded DNA. Like fluorophore-quencher molecular beacons (FQ-MBs) AgNC-based molecular beacons (AgNC-MBs) are based on a single-stranded DNA that undergoes a conformational change upon binding a target sequence. The new conformation exposes a stretch of single-stranded DNA capable of hosting a fluorescent AgNC upon reduction in the presence of Ag<sup>+</sup> ions. The utility of AgNC-MBs has been limited, however, because changing the target binding sequence unpredictably alters cluster fluorescence. Here we show that the original AgNC-MB design depends on bases in the target-binding (loop) domain to stabilize its AgNC. We then rationally alter the design to overcome this limitation. By separating and lengthening the AgNC-stabilizing domain, we create an AgNC-hairpin probe with consistent performance for arbitrary target sequence. This new design supports ratiometric fluorescence measurements of DNA target concentration, thereby providing a more sensitive, responsive and stable signal compared to turn-on AgNC probes. Using the new design, we demonstrate AgNC-MBs with nanomolar sensitivity and single-nucleotide specificity, expanding the breadth of applicability of these cost-effective probes for biomolecular detection.

Received 12th May 2016,  
Accepted 5th July 2016  
DOI: 10.1039/c6nr03827a  
[www.rsc.org/nanoscale](http://www.rsc.org/nanoscale)

### Introduction

Nucleic acid detection and quantification is a critical tool for molecular biology and clinical diagnostics as it can provide important genetic and regulatory information without the need for expensive and time-consuming sequencing. Synthetic nucleic acids with conjugated fluorescent dyes are among the most widely used probes owing to their availability, customizability and ease of use.<sup>1</sup> Fluorescence provides high sensitivity while sequence-dependent hybridization provides specific, separation-free detection.

Molecular beacons are a well-known example of hybridization-based fluorescent probes. They are comprised of a short oligonucleotide with fluorophore and quencher moieties conjugated to opposite ends.<sup>2,3</sup> In its native state, the probe adopts a stem-loop structure with the quencher held in close proximity to the fluorophore by the stem, quenching fluorescence emission. After the loop hybridizes with its complementary target DNA, the oligonucleotide adopts an extended conformation, separating the fluorophore and quencher and increasing the fluorescent signal.

Among the drawbacks of such fluorophore-quencher molecular beacons (FQ-MBs) are high background fluorescence and susceptibility of their organic fluorophores to photobleaching. Additionally, the bulky dyes can interfere with target hybridization and the two conjugations require multiple steps of purification, ultimately resulting in low yields at a high production cost.<sup>4–7</sup> One way to overcome these limitations is to replace the fluorophore and quencher with a pair of partially complementary DNA sequences that, when separated, stabilize a fluorescent silver nanocluster (AgNC).<sup>8,9</sup>

DNA-AgNCs are a new class of fluorophore composed of few-atom silver clusters stabilized by a short stretch of single-stranded DNA.<sup>10,11</sup> Their small size (<1 nm) falls well below

<sup>a</sup>Department of Mechanical Engineering, University of California Santa Barbara, USA

<sup>b</sup>Department of Physics and Program in Biomolecular Science & Engineering, University of California Santa Barbara, USA. E-mail: [jtdo@engineering.ucsb.edu](mailto:jtdo@engineering.ucsb.edu)

† Electronic supplementary information (ESI) available: Tables containing DNA sequences of probes and targets; fluorescence emission spectra of AgNC12-MB probes containing a 4-dT spacer between domains; comparison of ratiometric fluorescence emission of AgNC22-MB probes using UV excitation and visible excitation; emission intensities of the green and red AgNCs generated by AgNC22-MBs with and without target and excited using peak visible excitation. See DOI: 10.1039/c6nr03827a

‡ Present address: Department of Chemical & Biomolecular Engineering, University of California, Berkeley, CA, USA.

the Fermi wavelength of Ag (0.5 nm),<sup>12</sup> giving rise to molecular-like fluorescence emission with size-dependent spectra that can be tuned *via* the sequence of the DNA ligand.<sup>13</sup> Some DNA-AgNCs exhibit bright emission, good photostability, high quantum efficiency and biocompatibility. Their low-cost and easy synthesis make them an attractive alternative to common fluorophores, such as organic dyes and quantum dots, in the development of DNA probes.<sup>10,14,15</sup>

AgNC-generating molecular beacons (AgNC-MBs), which incorporate a AgNC stabilizing sequence into the stem of a hairpin DNA, have been demonstrated as a viable alternative to FQ-MBs, offering the same turn-on type of sensitivity without the need to conjugate fluorophore and quencher dyes.<sup>8,9</sup> AgNC-MBs are hairpin DNAs that, like FQ-MBs, contain a target binding domain within their loop. A sequence capable of stabilizing a fluorescent AgNC is contained within the hybridized stem, where base-pairing prevents cluster formation.<sup>16</sup> Once the probe hybridizes with its target and unfolds, the AgNC template sequence is freed from the stem and generates a fluorescent AgNC after binding Ag<sup>+</sup> and undergoing reduction by NaBH<sub>4</sub>. Low production costs, owing to the absence of conjugation and purification steps, as well as low-background fluorescence and bright fluorescence upon target-binding make AgNC-MBs an attractive alternative to FQ-MBs.

The first AgNC-MBs were designed for the sensitive and specific detection of hepatitis B DNA using a complementary sequence, and thrombin protein using an aptamer loop sequence.<sup>8</sup> Although the design appeared to be generalizable, our attempts to modify the loop sequence to detect other targets yielded mixed results.<sup>9</sup> Here, we identify the cause of this fragility and introduce a new design that is robust to changes in target sequence while retaining the exquisite sensitivity to single nucleotide polymorphism (SNP) characteristic of MBs.<sup>17</sup>

Our new design also makes a dramatic and practical improvement to signal stability by introducing ratiometric functionality. Ratiometric functionality has been leveraged by FQ-MBs for DNA detection,<sup>18,19</sup> cellular labeling,<sup>20</sup> and sensing of a wide variety of analytes.<sup>21</sup> We create AgNC-MB probes with distinct emission bands in the bound and unbound states, thereby providing an internal reference that improves sensitivity, stability and response time.

## Results and discussion

The original silver nanocluster molecular beacon (AgNC-MB) design,<sup>8</sup> herein referred to as NC12, consists of a synthetic DNA oligomer with three sequence domains (Fig. 1): (i) a 12-base AgNC-stabilizing domain, (ii) a 30-base target-binding domain, and (iii) a 7-base blocking domain. In its hairpin ('off') state, the AgNC-stabilizing domain binds the blocking domain, inhibiting cluster formation. Conversely, in its extended ('on') state, the AgNC-stabilizing domain is liberated from the blocking domain and, upon reduction in the presence of silver ions, stabilizes a fluorescent cluster.

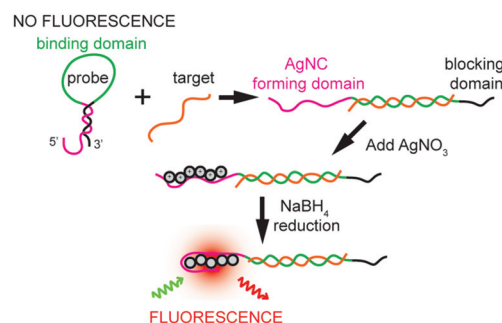


**Fig. 1** Schematic representation of silver nanocluster molecular beacons (AgNC-MBs). After binding to target, the hairpin unfolds to reveal an AgNC template sequence, which can then generate a fluorescent nanocluster.

In principle, as long as its number of bases and GC content remain the same, changing the target-binding sequence should not affect the operation of the probe.<sup>3</sup> However, replacing the 30 base Hepatitis B (HBV) target-binding domain of a functional NC12<sup>8</sup> with sequences complementary to targets for Hepatitis A (HAV) and Hepatitis C (HCV1)<sup>22–25</sup> yielded mixed results. As reported previously,<sup>9</sup> the HBV probe produced clusters with strong red fluorescence (600 nm) after binding target, but also produced a cluster in its hairpin state, with overlapping, albeit weaker, fluorescence emission peaked at 570 nm. The HAV probe worked best, producing clusters with a 600 nm peak emission when bound to target, and no fluorescence in the absence of target. However, the HCV1 probe produced clusters with a very weak fluorescence signal, peaked at both 570 nm and 650 nm, in the presence of target and much stronger fluorescence at 640 nm in the absence of target (Fig. 2c).

In search of a viable turn-on sensor for HCV, and to better assess the fragility of the NC12 design, we made probes for three other target sequences (HCV2, HCV3, HCV4) from the conserved region of the 5'-UTR for hepatitis C virus.<sup>23</sup> Only one, HCV3, yielded significant fluorescence after binding target (Fig. 2d). It fluoresced with peak emission at 640 nm after binding target, and also fluoresced in the absence of target, with similar emission, peaked at 630 nm, but reduced intensity. With only one in four NC12s for HCV proving viable as a fluorescent sensor, and two in five target-modified NC12s being viable overall, we estimate the NC12 design has a ~33% chance of producing a functional probe for an arbitrary target.

To rationally design a universal AgNC-MB probe, we sought to understand why the NC12 design fails to produce consistent AgNCs for different target sequences. The variety of AgNCs produced by the target-modified probes suggests that cluster formation depends on bases contained within the target binding domain. This is surprising considering that the 12-base AgNC-stabilizing domain is, by itself, capable of stabilizing a yellow-emitting cluster.<sup>26</sup> We note, however, that the emission of the AgNC produced by this 12-base sequence in isolation peaks at 540 nm, a wavelength 60 nm shorter than the peak emission of the HBV AgNC12-MB. One possible expla-

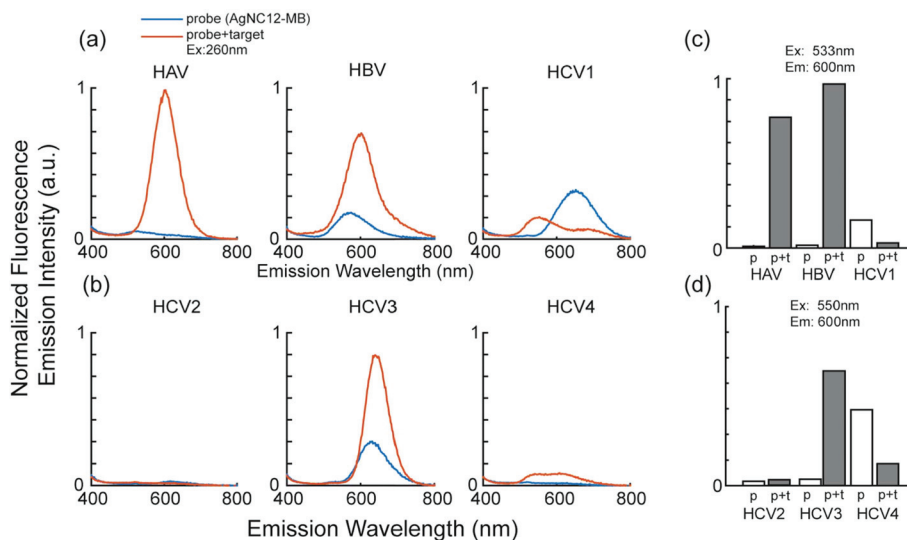


**Fig. 2** Fluorescence emission of AgNC12-MB probes for different target sequences. (a), (b) Fluorescence emission spectra of samples containing probes both with (blue) and without (red) target DNA under 260 nm illumination. (c), (d) Fluorescence emission intensity of AgNC12-MB probes under peak visible excitation illumination. Only HAV, HBV and HCV3 exhibit low background and high fluorescence enhancement after binding target. The fluorescence intensity of replicate samples varied by less than 10% in all cases.

nation for this discrepancy is that the 12-base oligomer produces clusters *via* formation of a homo-dimer, a common phenomenon for AgNCs stabilized using strands containing fewer than 16 bases.<sup>13,27,28</sup> A tendency of the 12-base sequence to recruit additional bases in order to form a cluster is also evidenced by its production of an AgNC with strong red fluorescence emission at 630 nm when in close proximity to a G-rich sequence.<sup>29</sup>

To test the hypothesis that proximity of the target-binding domain affects the function of the AgNC-stabilizing domain, we inserted four thymine bases (4T) into the DNA sequence between the two domains in the NC12 design. If bases contained within the 5'-end of the target binding domain participate in cluster formation, this insertion would destabilize the conformation of the bases and inhibit or alter cluster formation.<sup>30</sup> Doing so completely inhibited AgNC formation in the presence of target for all six target sequences tested (see ESI†), further supporting the notion that the 12-base AgNC-stabilizing sequence requires additional bases to stabilize a fluorescent AgNC.

We overcame this limitation and created an AgNC-MB that functions for arbitrary target sequences by redesigning the AgNC-MB to make AgNC-stabilization independent of the bases contained in the binding domain. Our new AgNC-MB design, herein referred to as NC22, replaces the 12-base AgNC domain of the original NC12 with a 22-base sequence attached to the target-binding domain *via* a 4T-linker. We chose this 22-base sequence because it is known to produce a bright red emissive cluster even when appended onto larger DNA structures through a 4T linker.<sup>31,32</sup> We then increased the length of the blocking domain from 7 to 10 bases to improve hairpin stability<sup>33</sup> and removed 5 bases from the 3' end of the target-binding domain to reduce overall probe length, thereby

decreasing the cost and increasing the chemical yield of the DNA strand synthesis.

To determine the ideal location for the blocking domain sequence, we characterized the fluorescence emission of three versions of NC22, each with a 10-base blocking domain complementary to a different portion of the AgNC-stabilizing domain. The three variants, shown schematically in Fig. 4, are labeled 5'-block, mid-block and 3'-block to indicate which region of the AgNC domain is blocked in the hairpin state. Using the HCV1 binding domain (which failed to produce a cluster bearing probe in the original NC12 design), we measured the fluorescence produced by each version of the NC22 design with and without added target. As expected, every version of the HCV1 NC22 produced an AgNC with red fluorescence when bound to target. The excitation and emission peaks closely match previous reports, suggesting the probe contains a cluster composed of 14 Ag<sup>0</sup> and a total charge of +8e due to the presence of unreduced Ag<sup>+</sup>.<sup>13</sup> However, each version of the probe differed in what it produced in the absence of target (Fig. 3). The 5'-block design produced AgNCs with bright red emission of similar spectra and intensity regardless of whether target DNA was present, making it a poor probe. The mid-block design also produced spectrally similar fluorescence with and without target, but significantly less fluorescence in the absence of target. It could therefore provide a 'turn-on' signal to indicate target binding, similar to the HAV NC12. Lastly, the 3'-block design produced a strong green fluorescence in the hairpin state, which is easily distinguished from the red fluorescence produced in the target-bound state. This green emitting AgNC presumably forms on the 12 bases (5'-TTCCCACCCACC-3') left unpaired at the 5' end of the AgNC-stabilizing domain the NC22 in the hairpin state. Excluding the first 2 Ts, this 10-base sequence is a sub-sequence of several 16-base oligomers known

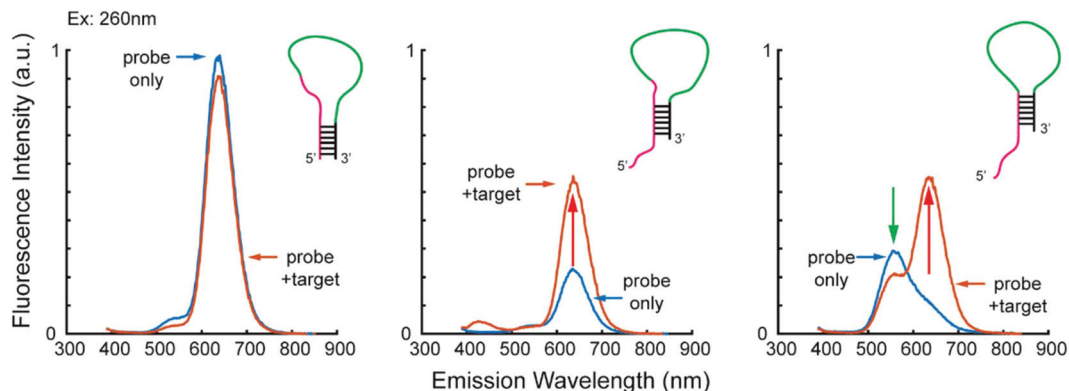


**Fig. 3** Fluorescence emission behavior of AgNC22-MBs with blocking domains complementary to different regions of the AgNC formation domain. Samples were excited using 260 nm illumination.

to stabilize fluorescent silver nanoclusters, albeit in homodimer form with near-infrared (nIR) emission.<sup>13,34,35</sup> The shorter wavelength emission of NC22 in its 'off'-state suggests that its cluster contains fewer silver atoms than those nIR-emitting clusters formed by related homodimers.

The two distinct AgNCs generated by the 3'-block-NC22 (shown schematically in Fig. 4a and b) enable a ratiometric measurement, proportional to the relative amounts of bound and unbound probe, which offers improved sensitivity, quantification and robustness to environmental variability.<sup>36</sup> In its hairpin form, the fluorescence produced by 3'-block-NC22 is predominantly from a green emitting AgNC with peak exci-

tation at 475 nm and peak emission at 550 nm (Fig. 4a). In the presence of an equimolar amount of target, the fluorescence is dominated by a red-emitting AgNC with peak excitation of 572 nm and peak emission of 640 nm (Fig. 4b). The ratio of red emission intensity to total emission intensity of the two fluorescence channels ( $F_R/(F_R + F_G)$ ) provides a ratiometric signal that increases in the presence of DNA target (Fig. 4c and d) regardless of the target-binding domain sequence. We observe a similar enhancement of the ratiometric signal when separately exciting the two AgNC emissions at their two visible excitation peaks as when exciting them simultaneously using 260 nm illumination (see ESI†).

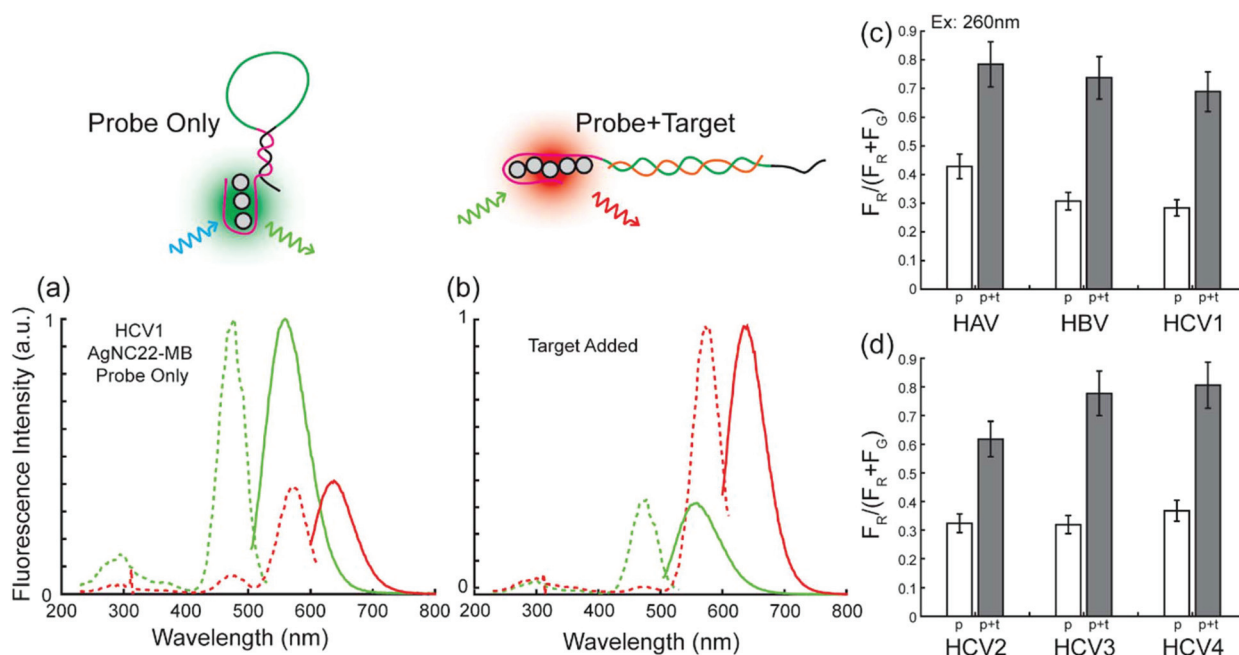


**Fig. 4** Schematic and fluorescence excitation and emission spectra of the HCV1 3'-block-AgNC22-MB in its (a) hairpin state where fluorescence is predominantly green (Peak excitation: 475 nm, emission: 550 nm) and (b) bound state with an equimolar concentration of target DNA where fluorescence is predominantly red (Peak excitation: 572 nm, emission: 640 nm). (c), (d) Ratiometric fluorescence emission (excitation: 260 nm) of the 3'-block-AgNC22-MB is universally enhanced in the presence of target for all sequences tested. Error bars represent 10% of the ratiometric signal, the maximum variation in sample intensity observed between replicate experiments.

To examine the properties of the ratiometric signal, we used visible peak excitation. We found the ratiometric signal is proportional to target concentration (Fig. 5a). Green fluorescence intensity decreases and red fluorescence intensity increases as target DNA concentration increases, while the ratiometric signal increases linearly. For 150 nM of probe, we calculated a limit of detection ( $3\sigma_{\text{STD,noise}}$ ) of 8.9 nM (Fig. 5b), comparable to the detection limit of typical fluorophore-quencher molecular beacons.<sup>37,38</sup>

Furthermore, the ratiometric measurement matured rapidly and was remarkably stable. This is especially notable because AgNC solutions must often incubate for hours after reduction before the intensity of their fluorescence begins to stabilize.<sup>30,39,40</sup> During this time, sample intensity increases and fluctuates as the clusters form and possibly undergo rearrangement and oxidize into different emissive species.<sup>41,42</sup> The AgNCs formed by 3'-block-AgNC22-MBs are no exception. Their absolute intensities increase by an order of magnitude

over 12 hours following chemical reduction (Fig. 5c). As a result, turn-on fluorescence assays based on the generation of fluorescent AgNCs require many hours of equilibration before a reliable measurement can be made. By contrast, the ratio of emissions from the two AgNCs that form on the 3'-block-AgNC22-MB stabilizes within minutes of chemical reduction and fluctuates less than 0.2% from its mean over the course of 12 hours (Fig. 5d). Thus, our ratiometric probe allows for rapid quantification almost instantly or at any point in time after chemical reduction.

The 3'-block-AgNC22-MB can be easily adapted to a diverse array of biologically and clinically relevant targets. For example, a 3'-block-AgNC22-MB made to bind the DNA analog of miRNA182 (a microRNA whose regulation and expression are relevant to various cancers, neurological disorders, and sepsis<sup>43-46</sup>) exhibited the same emissions and ratiometric qualities as the various hepatitis probes (Fig. 6a). The 3'-block-AgNC22-MB can also be used to discriminate between targets

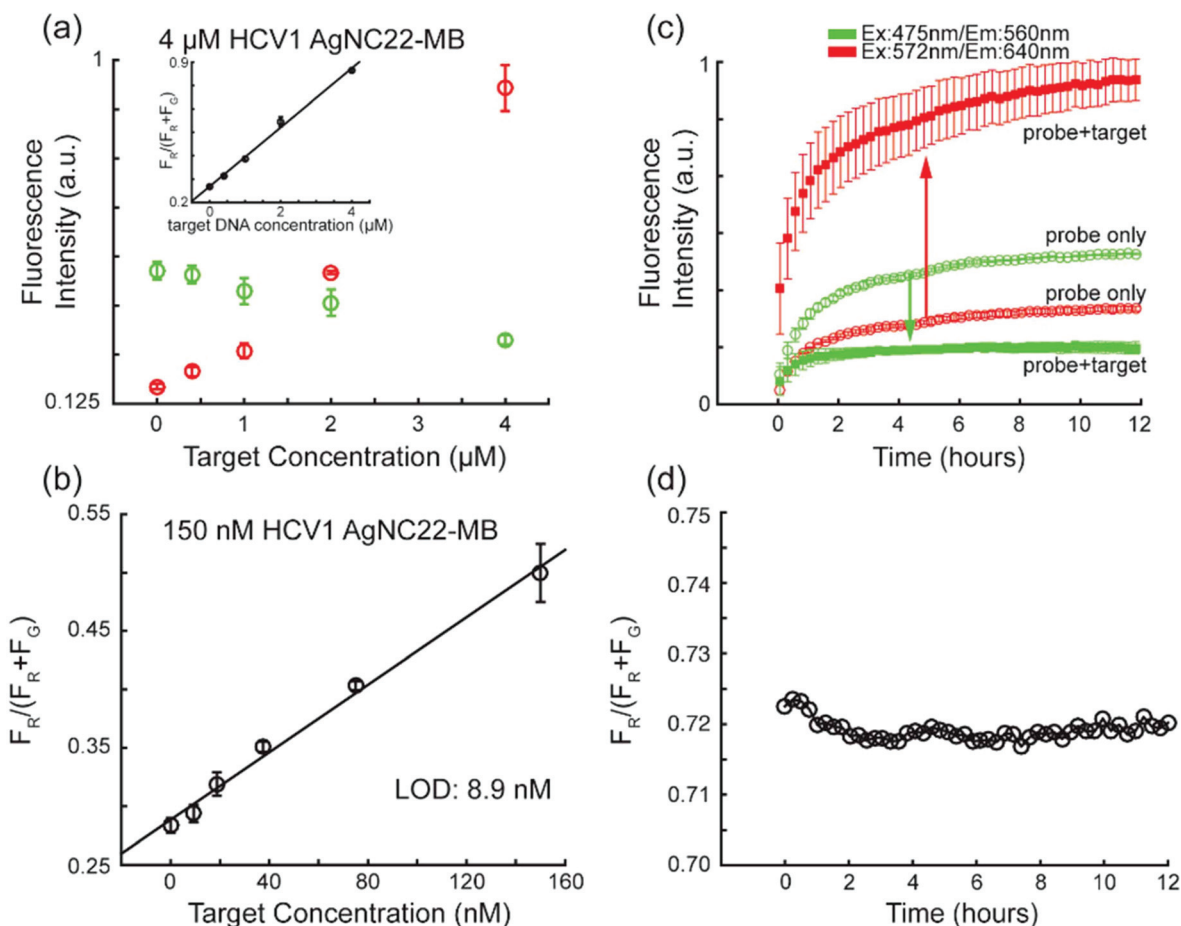


**Fig. 5** (a) Green and red fluorescence emission versus target concentration for sample containing 4  $\mu\text{M}$  of HCV1 AgNC22-MB. Inset: The ratiometric fluorescence ( $F_R/(F_R + F_G)$ ) varies linearly with target concentration. (b) Using 150 nM probe, the ratiometric fluorescence emission is sensitive (8.9 nM LOD) and linear. (c) Fluorescence intensity of HCV1 probe measured over time after addition of  $\text{NaBH}_4$ . Fluorescence intensity of red and green emission increases as the clusters mature over a 12 hour period. (d) The ratiometric fluorescence of the sample containing probe and target remains constant over time, with a variation of 0.2% from the mean, allowing for quantification within minutes. In all plots, error bars indicate the standard deviation of three replicate samples.

that differ by a single nucleotide. A 3'-block-AgNC22-MB designed to bind the *HRAS* gene containing an single nucleotide polymorphism (SNP) associated with a bladder cancer<sup>47,48</sup> successfully discriminated between mutant and wild-type targets (Fig. 6b) under optimized buffer conditions (see ESI†).

Although it improves upon previous AgNC-MBs, the 3'-block-AgNC22-MB still suffers drawbacks common to many AgNC based sensors. First, AgNC synthesis is sensitive to variations in buffer composition and pH, which limit the range of environments in which the sensor can be used in an assay. Also, because synthesis is performed after target binding, the sensor is not suited to real time monitoring of target production or *in vivo* monitoring of target concentration. Nevertheless, for rapid and sensitive target quantification under controlled *in vitro* conditions, this redesigned AgNC-MB provides a robust, low-cost and practical alternative to conventional, fluorophore-quencher MBs.

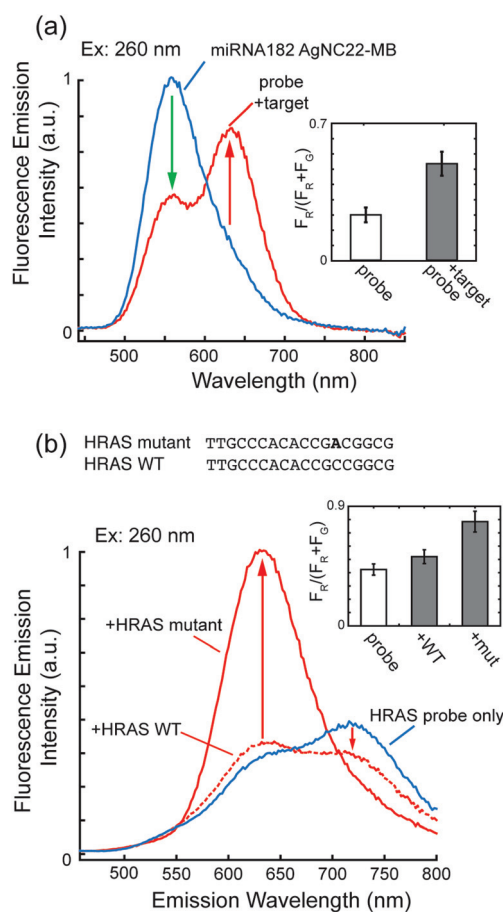


**Fig. 6** (a) Fluorescence emission of an AgNC22-MB probe for a DNA target of miRNA182 under 260 nm excitation. Inset: Ratiometric fluorescence signal of the probe increases in the presence of target. (b) Fluorescence emission of a mutant-selective AgNC22 probe for the *HRAS* gene. A decrease in fluorescence emission at 716 nm and an increase at 634 nm is observed in the presence of the mutant target, while negligible signal change occurs in the presence of the wildtype target. Inset: Ratiometric fluorescence signal of the *HRAS* NC22 probe for mutant and wildtype target.

## Experimental

### Preparation of silver nanoclusters

Probe and target DNA strands were purchased from Integrated DNA Technologies, Inc. (Coralville, IA, USA; <http://www.idtdna.com>) with standard desalting. Strands were rehydrated with 18.2 MOhm cm deionized water (DI, MilliQ, Millipore) and stored at 100–500  $\mu\text{M}$  at  $-20^\circ\text{C}$ . Sodium phosphate buffer was prepared as a 10 $\times$  stock at 200 mM at pH 7.5 by combining solutions of sodium phosphate monobasic monohydrate (Certified ACS, >98%) and sodium phosphate dibasic heptahydrate (Certified ACS, >98%) in MilliQ DI. pH was measured using an Oakton pH 11 series meter with dual junction electrode. Silver nitrate (ReagentPlus, >99.0%), sodium borohydride pellets (Aldrich, >99.99%), magnesium acetate tetrahydrate (BioXtra, >99%), and citric acid (ACS Reagent, >99.5%) were purchased from Sigma Aldrich.

AgNC generation using AgNC12-MBs was adapted from ref. 8 and 9 and performed as follows: frozen DNA stocks were allowed to thaw at room temperature, then vortexed. 3  $\mu\text{L}$  of 500  $\mu\text{M}$  probe was combined with 32.2  $\mu\text{L}$  of 20 mM sodium phosphate buffer. Probe and buffer were heated to 90  $^\circ\text{C}$  for 5 minutes and then snap cooled in an ice bath. 3  $\mu\text{L}$  of 500  $\mu\text{M}$  target (or 3  $\mu\text{L}$  of DI water for target-less control samples) was added to probe and buffer samples, vortexed and allowed to incubate at room temperature for 1 hour in the dark. Addition of 0.9  $\mu\text{L}$  of 10 mM  $\text{AgNO}_3$  to each sample was followed by an approximately 20 minute incubation at room temperature while a fresh solution of 2 mM  $\text{NaBH}_4$  in 0.1 mM  $\text{NaOH}$  was prepared. The  $\text{NaOH}$  was used to increase the pH and stabilize the  $\text{NaBH}_4$  during pipetting, which improved consistency from run to run.<sup>49</sup> Samples were reduced by adding 4.5  $\mu\text{L}$  of the sodium borohydride solution followed by vortexing. After reduction, samples were stored at room temperature in the dark until fluorescence characterization. Final concentrations were 34.4  $\mu\text{M}$  DNA, 206  $\mu\text{M}$   $\text{AgNO}_3$  and 206  $\mu\text{M}$   $\text{NaBH}_4$  ( $[\text{DNA probe}]:[\text{AgNO}_3]:[\text{NaBH}_4] = 1:6:6$ ).

AgNC generation using AgNC22-MBs was adapted from ref. 31 and prepared as follows: frozen DNA stocks were allowed to thaw at room temperature followed by vortexing. 1.5  $\mu\text{L}$  of 500  $\mu\text{M}$  probe was combined with 31.88  $\mu\text{L}$  of 20 mM sodium phosphate buffer. Probe and buffer were heated to 90  $^\circ\text{C}$  for 5 minutes and then snap cooled in an ice bath. 1.5  $\mu\text{L}$  of 500  $\mu\text{M}$  target (or 1.5  $\mu\text{L}$  of DI water for target-less control samples) was added to probe and buffer samples, vortexed and allowed to incubate at room temperature for 1 hour in the dark. Addition of 0.75  $\mu\text{L}$  of 10 mM  $\text{AgNO}_3$  to each sample was followed by an approximately 20 minute incubation at room temperature in the dark before chemical reduction using 1.88  $\mu\text{L}$  of 2 mM  $\text{NaBH}_4$  in 0.1 mM  $\text{NaOH}$  and vortexing. After reduction, samples were stored at room temperature in the dark until fluorescence characterization. The final concentrations were 20  $\mu\text{M}$  DNA probe, 200  $\mu\text{M}$   $\text{AgNO}_3$  and 100  $\mu\text{M}$   $\text{NaBH}_4$  ( $[\text{DNA probe}]:[\text{AgNO}_3]:[\text{NaBH}_4] = 1:10:5$ ). We obtained similar results using a modified procedure that maintained the same concentration ratios (10  $\mu\text{L}$  of 10  $\mu\text{M}$

probe, 10  $\mu\text{L}$  of 10  $\mu\text{M}$  target, 20  $\mu\text{L}$  of 20 mM buffer, 5  $\mu\text{L}$  of 0.2 mM  $\text{AgNO}_3$ , 5  $\mu\text{L}$  of 0.1 mM  $\text{NaBH}_4$ ). For sensitivity measurements, the final concentration of  $\text{AgNO}_3$  and  $\text{NaBH}_4$  were scaled with concentration of probe (4  $\mu\text{M}$  or 150  $\mu\text{M}$ ) to maintain the same concentration ratios. In the presence of 5 $\times$  excess of target DNA, probe samples failed to produce a fluorescent signal, presumably due to competition between probe and target for  $\text{Ag}^+$ .

For the *HRAS* gene probes, we included 7 mM citric acid and 2 mM magnesium acetate and raised incubation and reaction temperatures to 30  $^\circ\text{C}$  to improve discrimination between mutant and wildtype targets. We included magnesium acetate to optimize the relative melting temperatures of the probe and the two targets to improve discrimination.<sup>50</sup> We also found that for this case, addition of citric acid, which aids in the formation of other types of silver nanomaterials,<sup>51</sup> increased fluorescence intensity but changed the fluorescence emission of the clusters generated by the probe in its hairpin state from 550 nm to 716 nm. The clusters generated in the target-bound state were unaffected.

### Fluorescence spectroscopy

Fluorescence excitation and emission spectra and intensities were obtained using a Tecan infinite 200Pro plate reader with Tecan i-control software (Tecan Group Ltd) between 1 and 5 hours after chemical reduction of samples. The step size and bandwidth were set to 2 nm and 20 nm for emission scans, and to 5 nm and 5–10 nm for excitation scans and were performed using Top Mode. The gain was kept constant for characterization experiments (105 for 260 nm excitation and 75 for visible excitation). For sensitivity measurements, the gain was optimized for the samples containing the highest concentration of target and then held constant for remaining samples. For time series fluorescence data, 384-well plates (black, clear-flat bottom, Part 3540, Corning, Inc.) were covered with transparent tape and measured using Bottom Mode. Empty wells were also processed to check for autofluorescence of the wellplate and tape. Peak excitation and emission wavelengths were obtained by fitting Gaussian distributions using Matlab (The Mathworks, Inc.).

## Conclusions

We have rationally designed a universal, label-free DNA probe that generates spectrally distinct AgNCs in its bound and unbound states. The AgNC-MB probes that inspired our design behave unpredictably for different targets. We found this fragility is due to involvement of bases from the target-binding domain in cluster formation. By the introduction of a new AgNC-stabilizing domain, separated from the target-binding domain by a few dTs, and thoughtful placement of the blocking domain, our new AgNC-MB design produces one AgNC in its hairpin state that is spectrally well-separated from the AgNC it produces after binding to its target. AgNC-MB probes of this design behave similarly for all of the eight different

target binding sequences tested and are capable of discrimination between targets that differ by a single nucleotide under optimized buffer conditions. We note that the relative amount of target-bound AgNC fluorescence to target-free AgNC fluorescence is directly proportional to target concentration. The ratiometric measurement enabled by our new AgNC-MB design is thereby not only robust to changes in target sequence and buffer composition, it is also constant over time, allowing for quantification of target DNA concentration within minutes.

A major limitation of our AgNC-MB design is the requirement for AgNC synthesis post-target hybridization. Rational design of an MB-like construct which changes the environment of a pre-existing AgNC enough to detectably alter its emission spectrum for ratiometric sensing remains an important goal for research. Meanwhile, under conditions that allow AgNC synthesis after exposure to target, the design introduced here can serve as a convenient, robust and low-cost alternative to fluorescence-quencher type MBs for rapid DNA detection.

## Abbreviations

AgNC	Silver nanocluster
MB	Molecular beacon
SNP	Single nucleotide polymorphism
UTR	Untranslated region
HAV	Hepatitis A virus
HBV	Hepatitis B virus
HCV	Hepatitis C virus
miRNA	Micro RNA

## Acknowledgements

The authors would like to thank S. Copp, S. Swasey and E. Gwinn for discussions and advice. We acknowledge support from National Science Foundation grant NSF-CHE-1213895. This work was partially supported by the Institute for Collaborative Biotechnologies through grants W911NF-09-0001 and W911NF-12-1-0031 from the U.S. Army Research Office. The content of the information does not necessarily reflect the position or policy of the U.S. Government, and no official endorsement should be inferred. The authors acknowledge the use of the Biological Nanostructures Laboratory within the California NanoSystems Institute, supported by the University of California, Santa Barbara, and the University of California Office of the President.

## Notes and references

- 1 J. G. Wetmur, *Crit. Rev. Biochem. Mol. Biol.*, 1991, **26**, 227–259.
- 2 S. Tyagi and F. R. Kramer, *Nat. Biotechnol.*, 1996, **14**, 303–308.

- 3 K. Wang, Z. Tang, C. J. Yang, Y. Kim, X. Fang, W. Li, Y. Wu, C. D. Medley, Z. Cao, J. Li, P. Colon, H. Lin and W. Tan, *Angew. Chem., Int. Ed.*, 2009, **48**, 856–870.
- 4 D. M. Kolpashchikov, *Scientifica*, 2012, **2012**, 928783.
- 5 W. Tan, K. Wang and T. J. Drake, *Curr. Opin. Chem. Biol.*, 2004, **8**, 547–553.
- 6 H.-C. Yeh, J. Sharma, J. J. Han, J. S. Martinez and J. H. Werner, *Nano Lett.*, 2010, **10**, 3106–3110.
- 7 D.-L. Ma, H.-Z. He, K.-H. Leung, H.-J. Zhong, D. S.-H. Chan and C.-H. Leung, *Chem. Soc. Rev.*, 2013, **42**, 3427–3440.
- 8 Y. Xiao, Z. Wu, K.-Y. Wong and Z. Liu, *Chem. Commun.*, 2014, **50**, 4849–4852.
- 9 J. T. Del Bonis-O'Donnell, D. K. Fyngenson and S. Pennathur, *Analyst*, 2015, **140**, 1609–1615.
- 10 J. M. Obliosca, C. Liu and H.-C. Yeh, *Nanoscale*, 2013, **5**, 8443–8461.
- 11 J. T. Petty, J. Zheng, N. V. Hud and R. M. Dickson, *J. Am. Chem. Soc.*, 2004, **126**, 5207–5212.
- 12 J. Zheng, P. R. Nicovich and R. M. Dickson, *Annu. Rev. Phys. Chem.*, 2007, **58**, 409–431.
- 13 D. Schultz, K. Gardner, S. S. R. Oemrawsingh, N. Markešević, K. Olsson, M. Debord, D. Bouwmeester and E. Gwinn, *Adv. Mater.*, 2013, **25**, 2797–2803.
- 14 H.-C. Yeh, J. Sharma, I.-M. Shih, D. M. Vu, J. S. Martinez and J. H. Werner, *J. Am. Chem. Soc.*, 2012, **134**, 11550–11558.
- 15 J. M. Obliosca, M. C. Babin, C. Liu, Y.-L. Liu, Y. Chen, R. A. Batson, M. Ganguly, J. T. Petty and H. Yeh, *ACS Nano*, 2014, **8**, 10150–10160.
- 16 E. G. Gwinn, P. O'Neill, A. J. Guerrero, D. Bouwmeester and D. K. Fyngenson, *Adv. Mater.*, 2008, **20**, 279–283.
- 17 S. Tyagi and F. R. Kramer, *Nat. Biotechnol.*, 1996, **14**, 303–308.
- 18 S. Tyagi, S. A. Marras and F. R. Kramer, *Nat. Biotechnol.*, 2000, **18**, 1191–1196.
- 19 L. Liu, Q. Yang, J. Lei, N. Xu and H. Ju, *Chem. Commun.*, 2014, **50**, 13698–13701.
- 20 P. J. Santangelo, B. Nix, A. Tsourkas and G. Bao, *Nucleic Acids Res.*, 2004, **32**, e57.
- 21 M. H. Lee, J. S. Kim and J. L. Sessler, *Chem. Soc. Rev.*, 2015, **44**, 4185–4191.
- 22 J. S. Carneiro, M. Equestre, P. Pagnotti, A. Gradi, N. Sonenberg and R. P. Bercoff, *J. Gen. Virol.*, 1995, **76**, 1189–1196.
- 23 F. Moretti, F. Bolcic, L. Mammana, M. B. Bouzas, N. Laufer and J. Quarleri, *AIDS Res. Hum. Retroviruses*, 2010, **26**, 527–532.
- 24 N. Jothikumar, T. L. Cromeans, M. D. Sobsey and B. H. Robertson, *Appl. Environ. Microbiol.*, 2005, **71**, 3359–3363.
- 25 J. J. Germer, P. N. Rys, J. N. Thorvilson and D. H. Persing, *J. Clin. Microbiol.*, 1999, **37**, 2625–2630.
- 26 C. I. Richards, S. Choi, J.-C. Hsiang, Y. Antoku, T. Vosch, A. Bongiorno, Y.-L. Tzeng and R. M. Dickson, *J. Am. Chem. Soc.*, 2008, **130**, 5038–5039.
- 27 D. Schultz and E. G. Gwinn, *Chem. Commun.*, 2012, **48**, 5748–5750.
- 28 S. M. Copp, D. Schultz, S. Swasey, J. Pavlovich, M. Debord, A. Chiu, K. Olsson and E. Gwinn, *J. Phys. Chem. Lett.*, 2014, **5**, 959–963.
- 29 J. Li, X. Zhong, H. Zhang, X. C. Le and J.-J. Zhu, *Anal. Chem.*, 2012, **84**, 5170–5174.
- 30 P. Shah, A. Rørvig-Lund, S. Ben Chaabane, P. W. Thulstrup, H. G. Kjaergaard, E. Fron, J. Hofkens, S. W. Yang and T. Vosch, *ACS Nano*, 2012, **6**, 8803–8814.
- 31 D. Schultz, S. M. Copp, N. Markešević, K. Gardner, S. S. R. Oemrawsingh, D. Bouwmeester and E. Gwinn, *ACS Nano*, 2013, **7**(11), 9798–9807.
- 32 S. M. Copp, D. E. Schultz, S. Swasey and E. G. Gwinn, *ACS Nano*, 2015, **9**, 2303–2310.
- 33 A. Tsourkas, M. A. Behlke, S. D. Rose and G. Bao, *Nucleic Acids Res.*, 2003, **31**, 1319–1330.
- 34 J. T. Petty, C. Fan, S. P. Story, B. Sengupta, A. S. J. Iyer, Z. Prudowsky and R. M. Dickson, *J. Phys. Chem. Lett.*, 2010, **1**, 2524–2529.
- 35 J. T. Petty, C. Fan, S. P. Story, B. Sengupta, M. Sartin, J.-C. Hsiang, J. W. Perry and R. M. Dickson, *J. Phys. Chem. B*, 2011, **115**, 7996–8003.
- 36 P. Zhang, T. Beck and W. Tan, *Angew. Chem., Int. Ed.*, 2001, **40**, 402–405.
- 37 X. Liu and W. Tan, *Anal. Chem.*, 1999, **71**, 5054–5059.
- 38 X. Zuo, F. Xia, Y. Xiao and K. W. Plaxco, *J. Am. Chem. Soc.*, 2010, **132**, 1816–1818.
- 39 P. O'Neill, L. Velazquez, D. Dunn, E. Gwinn and D. K. Fyngenson, *J. Phys. Chem. C*, 2009, **113**, 4229–4233.
- 40 C. M. Ritchie, K. R. Johnsen, J. R. Kiser, Y. Antoku, R. M. Dickson and J. T. Petty, *J. Phys. Chem. C*, 2007, **111**, 175–181.
- 41 B. Sengupta, C. M. Ritchie, J. G. Buckman, K. R. Johnsen, P. M. Goodwin and J. T. Petty, *J. Phys. Chem. C*, 2008, **112**, 18776–18782.
- 42 J. T. Petty, S. P. Story, J.-C. Hsiang and R. M. Dickson, *J. Phys. Chem. Lett.*, 2013, **4**, 1148–1155.
- 43 M. Hanke, K. Hoefig, H. Merz, A. C. Feller, I. Kausch, D. Jocham, J. M. Warnecke and G. Sczakiel, *Urol. Oncol.*, 2010, **28**, 655–661.
- 44 K. Essandoh and G.-C. Fan, *Biochim. Biophys. Acta*, 2014, **1842**, 2155–2162.
- 45 O. C. Maes, H. M. Chertkow, E. Wang and H. M. Schipper, *Curr. Genomics*, 2009, **10**, 154–168.
- 46 Y. W. Kong, D. Ferland-McCollough, T. J. Jackson and M. Bushell, *Lancet Oncol.*, 2012, **13**, e249–e258.
- 47 E. P. Reddy, R. K. Reynolds, E. Santos and M. Barbacid, *Nature*, 1982, **300**, 149–152.
- 48 R. M. Franzini and E. T. Kool, *ChemBioChem*, 2008, **9**, 2981–2988.
- 49 D. A. Lyttle, E. H. Jensen and W. A. Struck, *Anal. Chem.*, 1952, **24**, 1843–1844.
- 50 R. Owczarzy, B. G. Moreira, Y. You, M. A. Behlke and J. A. Walder, *Biochemistry*, 2008, **47**, 5336–5353.
- 51 X. C. Jiang, C. Y. Chen, W. M. Chen and A. B. Yu, *Langmuir*, 2010, **26**, 4400–4408.